Touchless Palmprint Recognition and Its Evaluation on a Large-Scale Dataset

T

Xu Liang
https://orcid.org/0000-0003-4332-3494
The Chinese University of Hong Kong, Shenzhen, China

Chunsheng Zhang
https://orcid.org/0000-0002-6642-8996
The Chinese University of Hong Kong, Shenzhen, China

Wei Jia
Hefei University of Technology, China

David Zhang
The Chinese University of Hong Kong, Shenzhen, China

INTRODUCTION

Biometric recognition refers to using the inherent physiological or behavioral characteristics of the human body to perform personal identification. In general, physiological characteristics include palmprint, palm vein, palm dorsal vein, fingerprint, face, iris, retina, ear, knuckle print, lip print, voice print, etc., while behavioral characteristics include gait, signature, keyboard typing, and so on. With decades of development, biometric recognition has been widely used in everyday life.

Palmprint recognition is a member of the biometric recognition family. It is a technology that uses the unique features of the palm surface for biometric identification. As shown in Figure 1, the palm contains a wealth of features such as palm shape, principal lines, wrinkles, ridges, minutiae, textures, subcutaneous palm vein, and three-dimensional (3-D) surface curvatures.

Advantages of Palmprint Recognition

Among biometric recognition methods, face recognition has problems in situations, such as covering with a mask or goggles, and similar faces between identical twins; fingerprint recognition has issues of counterfeits, wet/dry fingers, and workers and elders who cannot offer clear fingerprints because of years of manual labor or problematic skins. Compared with these recognition methods, palmprint recognition has the advantages of high accuracy, high anti-counterfeiting capability, low privacy sensitivity, and low risk of germ transmission when considering public health, especially during the global COVID-19 pandemic. The prominent palmprint recognition with varieties of advantages has attracted a wide range of attention from academia and industry in recent years (Fei et al., 2018; Zhong et al., 2019).

DOI: 10.4018/978-1-6684-7366-5.ch047

Figure 1. Sample images of the palmprint and its features

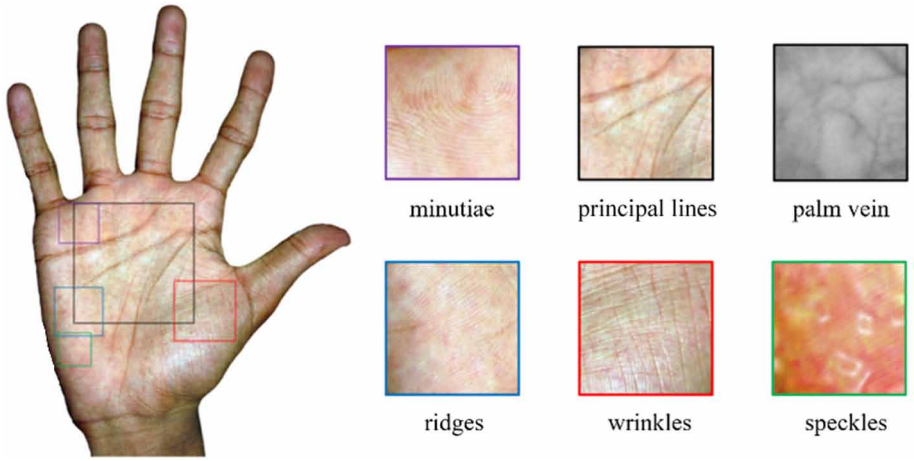

Categories of Palmprint Recognition

According to different criteria, palmprint recognition can be divided into different categories. Considering the palmprint image dimensions, it can be divided into two-dimensional (2-D) and 3-D palmprint recognition. When taking image resolution as a criterion, it can be divided into high-resolution and low-resolution categories (Zhang & Shu, 1999). According to whether the hand touches the capture device or not, it can be divided into touch-based and touchless palmprint recognition (TLPR). Along with the practical requirements, TLPR is more convenient and flexible. With more attention being paid to it, numerous kinds of TLPR systems have been proposed (Genovese et al., 2014; Zhang et al., 2017; Liang, Guo et al., 2021; Liang, Lu et al., 2022) and it has become the cutting-edge subject of palmprint recognition.

Application Scenarios

Due to the attractive advantages, low-resolution palmprint recognition is expected to have a wide range of practical applications. For instance, in the medical field, TLPR can avoid secondary pollution when identifying doctors and patients; In the traffic control field, TLPR can be applied in scenarios such as personal identification for intelligent turnstiles; In the field of finance with high secrecy and security demands, the effective anti-counterfeiting characteristics of TLPR can significantly improve the security of personnel authorization. Furthermore, in law enforcement agencies, TLPR can provide secure verification of personnel in scenes such as weapons and ammunition management. In contrast, high-resolution palmprint recognition is of much prospect in forensic applications, where partial-to-full matching is performed. For example, the latent palmprint obtained from knife hilts, gun grips, steering wheels, or glass surfaces from the crime scene, can be used to match against a registered database of full palmprints. However, due to complex backgrounds, small overlap regions, and a large number of detail features (e.g., creases and minutiae), latent palmprint matching is more challenging than the full-to-full template matching used in low-resolution palmprint recognition (Jain & Feng, 2008).

Organization of This Chapter

The most challenging issues of TLPR are lacking of large-scale dataset, and the imperfect palm postures and low-quality imaging caused by unconstrained acquisition modes and complex ambient lighting conditions. For the TLPR research, there is a strong requirement of unconstrained large-scale palmprint datasets. However, existing publicly available palmprint datasets, such as PolyU (The Hong Kong Polytechnic University [PolyU], 2009), Tongji (Zhang et al., 2017), and IITD (IIT Delhi, 2008), are all small-scale; thus, they are insufficient to demonstrate the generalization performance of the TLPR methods. To address the issues mentioned above, this chapter introduces a new multi-biometric database named "CUHKSZ" and then conducts a series of experiments on it to evaluate the TLPR performances for future reference.

The whole structure of this chapter is as follows. In section 2, the background of TLPR including issues and challenges are explored. Section 3 describes the newly established CUHKSZ dataset and introduces the classic palmprint recognition method CompCode (Kong & Zhang, 2004). In section 4, a series of experiments on the CUHKSZ dataset are performed to explore the optimal solutions and recommendations for TLPR. Section 5 highlights the future research directions of palmprint recognition. Finally, section 6 concludes this chapter.

BACKGROUND

A typical TLPR system consists of two components: image sensing and identity recognition. In detail, the recognition method includes palm region segmentation, keypoint detection, region of interest (ROI) localization, feature encoding, feature matching, and decision (Kong et al., 2009). According to the above components, the challenges in TLPR can be divided into two categories: image sensing-related and recognition method-related.

Issues and Challenges in Image Sensing

For TLPR, the whole palm region should be captured in image sensing. As a result, the target region is larger than the fingerprints and the palmprint feature scale is smaller than faces. Therefore, at the same camera resolution, it makes the pixel per inch (PPI) of the palmprint be more difficult to guarantee compared with fingerprint and face acquisitions, which gives rise to the problem that the palmprint features such as ridges and minutiae are often lost in the sensing process. Moreover, the face acquisition distance is above 30 cm, while the palm is around 10 cm to 20 cm from the device. Thus, motion blur and drastic changes in brightness occur more frequently in the process of palmprint imaging compared with that of face acquisition with a longer distance.

In general, palmprint sensing issues can be summarized into the following categories: (1) illumination problems such as over-bright, over-dark, or uneven lighting; (2) blur problems caused by defocusing, hand motion, or insufficient PPI; (3) geometric deformation problems such as perspective distortions caused by palm tilt, and radial or tangential distortions caused by camera lens; (4) information loss caused by palm stains, skin damage, or high image compression rate; (5) false information such as pseudo-edges caused by uneven illumination or palm distortion. The above factors will lead to difficulties in high-quality palmprint image sensing.

Accordingly, palmprint imaging has challenges in the following two aspects:

Optimum Design of Sensing Device. The palmprint sensing device should acquire a fine-grained palmprint pattern. To meet this requirement, the image resolution of the sensing device should be ensured to be high. In addition, due to the short acquisition distance, the movement of the palm will cause significant fluctuations in image brightness and sharpness, which brings great challenges to the general 3A (i.e., automatic exposure, automatic white balance, and automatic focus adjustment) methods of the camera's image signal processor (ISP). Thus, a powerful sensing device with the ability to automatically adjust its parameters to overcome these problems and generate high-quality images is highly expected.

Palmprint Image Quality Assessment (IQA). Palmprint image quality assessment is an essential basis for palmprint recognition. It refers to the quantitative evaluation of image quality based on the characteristics of palmprint, such as brightness, sharpness, and illumination uniformity. In the process of palmprint acquisition, focus and illumination problems may occur due to a variety of palm postural changes, resulting in a loss of palmprint feature information. To overcome this problem, on the one hand, the palmprint IQA result should be fed back into the device to improve the quality and stability of its imaging. On the other hand, by providing the assessment result to the recognition algorithm, dynamic adjustments of the algorithm parameters or decision schemes can be realized to improve the final accuracy.

Issues and Challenges in Recognition Method

For TLPR, the palm images are acquired in unconstrained environments, leading to sensing problems such as palm pose variations (e.g., palm twist, tilt, finger closure, and spatial position change) and low-quality imaging (abnormal illumination and image blur). These issues make it be a challenging work for recognition algorithms to deal with intra-class variations and inter-class similarity.

For intra-class variation, above sensing problems make the ROI images from the same palm no longer be similar enough and will lead to misalignments of the ROI localizations. Thus, it may cause failures of global feature template matching or obtaining too few keypoint matches between ROI images. As a result, the issues increase the system's false rejection rate (FRR) between intra-class samples and thus seriously reduce the user experience.

For inter-class similarity, above sensing problems lead to the loss of palmprint detailed features, which will cause mismatching of principal lines or local texture features between inter-class samples, increasing the false acceptance rate (FAR) of the system. This highly affects recognition accuracy and system security.

Based on the above analysis, the challenges in the recognition method are in the following two aspects:

ROI Localization and Alignment. Compared with touch-based palmprint images, touchless palmprint images have more complex backgrounds. Accordingly, palm region segmentation is a critical step in TLPR. The segmentation quality directly affects the precision of the subsequent palm edge detection and ROI localization results. ROI localization is the prerequisite for palmprint recognition; the localization precision directly affects the distribution consistency of intra-class features (Liang et al., 2023). As a result, the location error will increase the system FRR, reduce the pass rate of the registered users, and seriously affect the user experience. Most palmprint ROI localization methods rely on keypoint detection; however, palm edges become not obvious in complex environments, and the hand pose also has a high

degree of freedom. These factors make the conventional keypoint detection algorithm unstable in touchless scenarios. Therefore, high precision and robust palm keypoint localization have become a severe challenge in TLPR. In addition, due to the complexity of practical application scenarios, multimodal-based fusion recognition (e.g., palmprint and palm vein) has become an inevitable choice to achieve robust segmentation and high anti-spoofing ability. However, due to the differences in positions and poses of the multi-view cameras, the palm regions in multimodal images are not aligned, and the nonlinear offset is related to the spatial position (x, y, z) of the palm. Therefore, how to align the ROIs in multimodal palmprint images is an urgent problem to be solved.

Robust Feature Representation and Multimodal Fusion. In TLPR, with the continually increasing data size, the number of hard samples increases synchronously. The similarity between inter-class samples and variation between intra-class samples will continue to deteriorate. Therefore, in the recognition step, the designed feature representation algorithms should make the matching distances between inter-class samples significantly larger than those of the intra-class samples. TLPR uses features such as principal lines, wrinkles, local textures, minutiae, and palm vein for biometric recognition, so there is a promising way to design a reliable multi-modal feature space to efficiently fuse multi-class features to increase the generalization performance of feature representation.

CUHKSZ MULTI-BIOMETRIC DATASET AND THE COMPCODE SCHEME

Data is the foundation of biometrics research. As a promising dataset for cutting-edge TLPR research in the biometrics community, fisrt, it should be collected in unconstrained environments to simulate the image sensing issues exist in real-world scenarios. Second, the large-scale property is also required for better exploring the intra-class variation and inter-class similarity problems for recognition. Motivated by it, a multi-biometric dataset CUHKSZ is established with the support by Natural Science Foundation of China under Grant 62172347.

As one of the most widely used benchmark methods for palmprint recognition, CompCode (Kong & Zhang, 2004) will be introduced as a representative method to test recognition performances on the CUHKSZ dataset.

CUHKSZ Multi-Biometric Dataset

CUHKSZ is a subject-aligned large-scale multi-biometric database comprising 10,000 subjects with their palmprint, face, and fingerprint biometrics images. Typical images of each biometric modal are shown in Figure 2. Because the topic of this chapter mainly focuses on TLPR, the CUHKSZ palmprint dataset is introduced in more detail.

As is shown in Figure 3, the CUHKSZ palm images were collected by a touchless bimodal sensing device comprising dual-band light sources, a binocular CMOS camera module with dual-band filters, and a TOF ranging sensor (Liang, Lu et al., 2022). The TOF ranging sensor can show the height of the palm from the device in real-time. Considering that the height of the palm to the device varies during the acquisition process, subjects were guided to put their palms in two different distance ranges (8-10 cm and 10-12 cm) from the device. For each distance range, three of each palmprint and palm vein image are captured simultaneously. In summary, this dataset provides six palmprint images and six palm vein images for each palm with 10,000 subjects, and the image resolution is 640×480.

Figure 2. Typical images of each biometric modal in the CUHKSZ subject-aligned large-scale multi-biometric dataset. From top row to bottom row, they are touchless palmprint images, touchless palm vein images, fingerprint images, and face images. Note that, for the sake of personal information safety, the modal images shown above are selected from different individuals; in addition, the faces are blurred out.

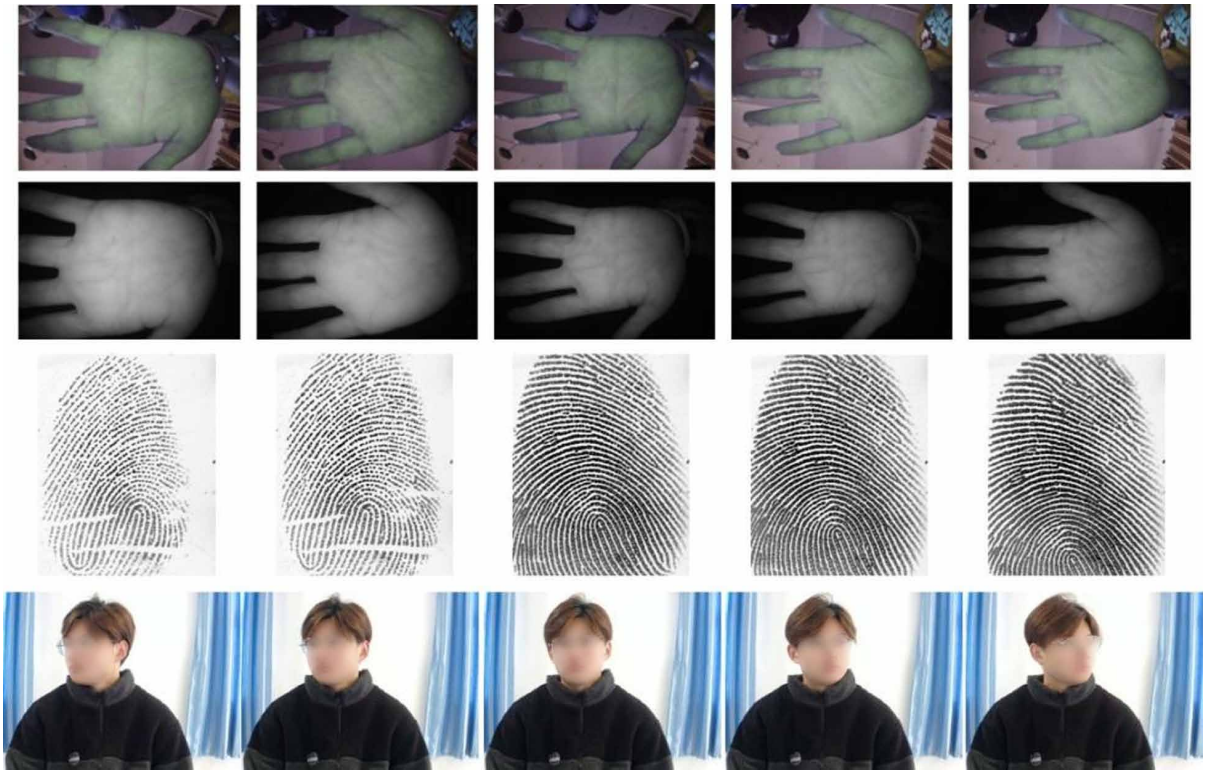

Figure 3. The CUHKSZ touchless palmprint and palm vein acquisition system

A brief comparison between the newly established CUHKSZ bimodal touchless palmprint dataset and the most used publicly available palmprint datasets is listed in Table 1. The statistics show that the CUHKSZ is the largest one among the existing palmprint datasets, with a difference of two orders of magnitude in scale.

Table 1. Comparison between the existing touch-based and touchless palmprint datasets

Datasets	Modal[a]	Sensing Mode[b]	No. of Hands	No. of Images	No. of Sessions
PolyU (PolyU, 2003)	PP	T	386	7,752	2
PolyU-MS (PolyU, 2009)	MS	T	500	24,000	2
CASIA (Chinese Academy of Sciences, 2005)	PP	TL	624	5,502	1
CASIA-MS (Chinese Academy of Sciences, 2007)	MS	TL	200	7,200	2
COEP (COEP Technological University, 2010)	PP	TL	163	1,305	1
FCPD (Liang, Guo et al., 2021)	PP, PV, D	TL	210	10,470	1
GPDS (University of Las Palmas de Gran Canaria, 2011)	PP, PV	TL	100	2,000	1
IITD v1.0 (IIT Delhi, 2008)	PP	TL	460	2,601	1
KTU Contactless (KTU CVPR Lab., 2015)	PP	TL	145	1,752	1
REST (Charfi et al., 2021)	PP	TL	358	1,948	1
Tongji (Zhang et al., 2017; Zhang et al., 2018)	PP, PV	TL	600	12,000	2
11K Hands (Afifi, 2019)	PP	TL	380	11,076	1
CUHKSZ	PP, PV	TL	20,000	120,000	1

[a]: PP represents palmprint, PV represents palm vein, MS represents multispectral palmprint images, and D represents depth information of the palm surface.

[b]: T as touch-based sensing mode, while TL as touchless sensing mode.

Competitive Code

The most significant feature of palmprint is the orientations of the line patterns. Thus, most palmprint recognition algorithms (Kong & Zhang, 2002; Jia et al., 2012; Liang, Yang et al., 2021; Jia et al., 2017) attempt to extract and encode the orientation information of palmprint patches. Among them, CompCode (Kong & Zhang, 2004) is the most classic one. It uses directional Gabor filters to extract line responses of a palmprint local region along different directions via convolution. And then encode the index of the direction in which the convolution obtained the maximum response. The 2D Gabor function used in this method is as follows:

$$\psi(x, y, x_0, y_0, \omega, \theta, \kappa) = \frac{-\omega}{\sqrt{2\pi}\kappa} e^{\frac{-\omega^2}{8\kappa^2}(4x'^2 + y'^2)} (\cos(\omega x') - e^{-\frac{\kappa^2}{2}}) \quad (1)$$

where $x' = (x - x_0)\cos\theta + (y - y_0)\sin\theta$, $y' = -(x - x_0)\sin\theta + (y - y_0)\cos\theta$. Note that only the real part is utilized to extract line patterns. Here, (x_0, y_0) is the function center and θ is the orientation of this Gabor function (in unit of radians). In addition, ω is the radial frequency (in unit of radians per

length) and δ is the half-amplitude bandwidth of the frequency response. Then, κ and ω can be obtained by:

$$\kappa = \sqrt{2\ln 2}\left(\frac{2^{\delta}+1}{2^{\delta}-1}\right) \tag{2}$$

and $\omega=\kappa/\sigma$ respectively.

In CompCode, six orientations are used to construct a Gabor filter bank, i.e., $\theta i = i\pi/6$, $i\in\{0,1,\ldots,5\}$, where θi is the orientation angle of the i-th Gabor filter. Then, six responses can be obtained after convoluting the ROI image by each directional filter in the Gabor filter bank, respectively. The competitive coding scheme is defined as follows:

$$i = \arg\max_{\theta}\{I(x,y) * \psi(x,y,\theta)\} \tag{3}$$

where I is the palmprint image, (x,y) *is* the pixel coordinate, ψ is the 2D Gabor filter obtained using Equation (1), θ is the orientation angle of ψ, and * denotes the convolution operator. Here, $i\in[0,5]$ denotes the orientation index in which the convolution response reaches the maximum, i.e., the winning index. Using a sliding window to filter the given palmprint ROI image with a fixed stride, the winning orientation index of each image patch (centered at the sample point) can be obtained. Finally, the winning indices will be utilized to construct the 2D feature template.

In the matching phase, the distance between two palmprint feature templates is measured by the average of the summation of the angular distances between two corresponding winning indices. In addition, the angular distance of two indices is defined in Table 2. To speed up the distance calculation process, the winning index i is represented by 3 bits (see Table 3). Combining Table 2 and Table 3, we can see that the well-designed bit representations make it possible to calculate the angular distance by performing XOR operations on the two 3-bit winning indices. Since on the CPU, the XOR instructions performed much faster than the arithmetic instructions, this coding scheme can significantly improve the speed of feature matching.

Table 2. All possible angular distances (α) between winning indices i1 and i2

i_2 \ i_1	**0**	**1**	**2**	**3**	**4**	**5**
0	0	1	2	3	2	1
1	1	0	1	2	3	2
2	2	1	0	1	2	3
3	3	2	1	0	1	2
4	2	3	2	1	0	1
5	1	2	3	2	1	0

Table 3. Bitwise representation of the Competitive Code

Winning index	**Bit 1**	**Bit 2**	**Bit 3**
0	0	0	0
1	0	0	1
2	0	1	1
3	1	1	1
4	1	1	0
5	1	0	0

The key hyper-parameters in the feature encoding phase are the size of the Gabor filter, the number of orientations of the filter bank, and the stride of the convolution sliding window. Considering the extracted ROI still contains localization errors caused by non-rigid deformations of the palm, in the feature matching phase, one of the two feature templates should be shifted and rotated to search for the best overlap region between the two ROIs. Accordingly, the key hyper-parameters in the feature matching phase are the ranges of template translations and rotations.

SOLUTIONS AND RECOMMENDATIONS

In this section, solutions and recommendations of TLPR are conducted from the following three aspects:

- The parameters optimization experiment of the representative CompCode (Kong & Zhang, 2004) method is performed to reveal the performance-changing trend and the optimal parameters set on the CUHKSZ palmprint dataset.
- A comparative study of some of the most widely used TLPR methods is conducted, which demonstrates the generalization capability of TLPR on large-scale datasets and provides benchmarks for future palmprint recognition research.
- The recognition performances of the three widely used biometrics, i.e., palmprint, face, and fingerprint, are evaluated. The experimental result shows the advantages of TLPR in terms of recognition accuracy, which provides a technical reference for civil applications.

Experimental Settings

Implementation. The experiments are carried out on a server with 160 Intel Xeon Gold 6230 CPUs and 337G RAM. All the ROI images are normalized and resized to 128×128. No data augmentation is leveraged in this experiment. CompCode (Kong & Zhang, 2004) is implemented by Matlab. By default, in the encoding stage, this chapter uses a directional Gabor filter bank with 6 orientations and the filter size is 35×35. In the matching stage, the translation shift pixels is set to [−3, 3] steps, and no template rotation is performed.

Performance Measures. The followings are standard metrics used for analyzing the accuracy and performance of a palmprint recognition system.

- Genuine Acceptance Rate (GAR) or True Acceptance Rate (TAR): The probability of the number of accepted attempts made by the genuine samples to the total number of attempts made by the genuine samples.
- False Acceptance Rate (FAR): The probability of the number of accepted attempts made by the impostor samples to the total number of attempts made by the impostor samples.
- False Rejection Rate (FRR): The probability of the number of rejected attempts made by the genuine samples to the total number of attempts made by the genuine samples.
- Equal Error Rate (EER): When FAR equals FRR, the value of FAR or FRR is the EER, i.e., EER = FAR = FRR.
- Receiver Operating Characteristic (ROC) curve: A metric to evaluate the output quality of a binary classifier. ROC curve typically plots GAR on the Y axis, and FAR on the X axis.

- Detection Error Tradeoff (DET) curve: DET curve typically plots FRR on the Y axis, and FAR on the X axis.
- Rank-1 accuracy: The probability that a sample is correctly recognized using the nearest neighbor classifier.

Evaluation Protocols. It is well known that there are two recognition modes for a biometric system, i.e., identification and verification (Zhang et al., 2003). For palmprint verification, the EER can be obtained based on the intra-class and inter-class matching scores. For palmprint identification, after matching with all the classes in the enrollment set, the label of the probe palm can be predicted using the nearest neighbor classifier. Then, the rank-1 accuracy rate can be calculated by the mean correct rate of the predictions obtained from the test set.

This chapter uses EER as the main evaluation metric, because most existing palmprint recognition methods are designed for person verification. Considering the real applications of palmprint verification, the matching scheme used in the works of Liang, Lu et al. (2022), Matkowski et al. (2019), and Genovese et al. (2019) is adopted to providw a comprehensive evaluation and comparison of different palmprint verification algorithms. Specifically, for each palm, the scheme takes 3 images for enrollment and the remaining images for testing. Thus, the matching is performed between a test image and the 3 corresponding registered images, where the minimum distance of the three distances is used as the final matching score for the current category in the registration set.

CompCode Optimization

CompCode extracts the orientation information from the palm lines and stores it in the competitive code template based on the well-designed bit planes. Then, the average angular distance method, implemented by a lookup table, is developed to effectively calculate the dissimilarity score between two competitive code templates. CompCode has been widely used because it achieves excellent performance both in execution speed and recognition accuracy. In addition, the feature template extracted from one ROI image only costs 512 bytes. However, the results of existing studies were obtained from small-scale datasets. Thus, it is insufficient to demonstrate their effectiveness in real-world applications.

In this section, performance evaluation and parameter optimization of CompCode are conducted on the newly established CUHKSZ palmprint dataset (only the palmprint modal is implemented). More specifically, the performance evaluation of CompCode is mainly tested by changing the values of three parameters: the number of Gabor filter banks (denoted k) in the feature encoding stage, and the template translation shift steps (denoted t) and rotation angles (denoted r) during feature matching stage.

Influence of the number of Gabor filter orientations. The number of Gabor filter banks is associated with the expressivity of the model, which is the capacity to effectively and discriminatively represent the palmprint image. Specifically, this chapter evaluates the Gabor filter banks by changing the number of Gabor orientations and conducts the performance analysis on the CUHKSZ palmprint dataset. As is shown in Table 4, when the Gabor orientations is 6, CompCode achieved the lowest EER. Note that the range of translation is fixed as 3 and the rotation angle is set to be 0 during matching.

Table 4. Palmprint verification EER (%) obtained by CompCode using different number of orientations

Filter Bank Orientations (*k*)	4	6	8
Palmprint	0.1746	**0.1616**	0.1658

Influence of template shift steps. The translation shift procedure during the matching stage means vertically and horizontally translating one feature template of the matching pair in the range of [−t, t] steps to calculate their similarity select the maximum similarity score as their final mathcing result. Thus, this parameter can affect the robustness against variations within intra-class palms. Table 5 illustrates the performance of CompCode with different translation shift steps, the value varies from 1 to 6. Here, one shift step of feature template means 3 pixels shift in the original ROI image. Hence, t = 6 means the ROI will be shifted from -18 pixels to +18 pixels to search for the best overlap region of the two ROIs. As is shown in Table 5, the translation shift steps of 6 is preferred, CompCode achieved the lowest EER on CUHKSZ dataset. Note that the number of orientations in the Gabor filter bank is fixed as 6 and the rotation angle as 0.

Table 5. Parameter analysis (report EER (%)) of translation shift steps based on CompCode

Shift Steps *t*	1	2	3	4	5	6
Palmprint	1.7292	0.4024	0.1616	0.1023	0.0759	0.0706

Influence of template rotation angles. Based on the fact that in the touchless palmprint data acquisition, there is no panel for palms to fix the height and direction, so the palm placement may show different heights and angles. Accordingly, this section mainly focuses on the influence of template rotation angles and conducts two series of experiments.

The first series is CompCode with rotations [-2^o, 0^o, $+2^o$] and [-3^o, 0^o, $+3^o$]. Rotation range of [-2^o, 0^o, $+2^o$] means the Gabor template of a test palm image will be rotated at a fixed angle of -2^o and $+2^o$ to obtain two rotated templates, and the template not rotated is also preserved. In the matching stage, these three templates will be matched with multiple features of each palm in the database, the best matching score is regarded as the matching result. The scheme of [-3^o, 0^o, $+3^o$] is likewise. Table 6 demonstrates the CompCode performance with different rotation angles, which shows that CompCode without rotations obtained the best EER result.

Table 6. EER (%) obtained by CompCode using different rotation ranges

Rotation Angles	0°	[-2°, 0°, 2°]	[-3°, 0°, $+3^\circ$]
Palmprint	0.0759	0.0962	0.1447

The second series is CompCode without rotation and with fixed rotation angles, i.e., [-3^o, 0^o, $+3^o$] under different shift steps. As shown in Table 7, it is obvious that CompCode without rotation achieves the best EER. The reason for the above phenomenon is that the ROI localization algorithm has already coarsely aligned the palm rotations. Therefore, template rotation may increase the similarity between inter-class features, bring a negative influence on the final recognition accuracy. In this experiment, the number of Gabor filter orientations is fixed to be 6.

Table 7. The performance of CompCode (report EER (%)) with different translation shift steps and rotation angles

Steps (t) / Angles (r)	1	2	3
0°	1.7292	0.4024	0.1616
[−3°, 0°, +3°]	1.7461	0.4498	0.2082

Time consumption analysis. Based on previous experimental results, the template rotation angle has no obvious contribution to the recognition performance. Thus, this section only conducts detailed experiments by changing the numbers of Gabor filter orientations (k) and translation shift steps (t) in this experiment. The code is implemented in Matlab using 72 parallel threads.

Table 8 shows the EER obtained using the CompCode with different shift steps and the number of Gabor filter orientations on the CUHKSZ dataset. As can be seen, the CompCode obtains the best performance when taking translation shift steps of 5 (corresponding to 15 pixels in the 128×128 ROI image) and Gabor filter banks with 6 orientations. And also, with the increasing translation shift steps the performance gets better. When the translation shift steps reaches 5, the performance remains stable when the number of the Gabor filter orientations is 6; then, increasing the number of Gabor filter banks results in no better performance.

Table 8. EER (%) and total matching time consumption (hour) obtained by CompCode using different numbers of Gabor filter orientations (k) and translation steps (t) on the entire CUHKSZ touchless palmprint dataset

Orientations k / Steps t	4	6	8	Matching Time (h)
1	1.9208	1.7292	1.6665	5.2
2	0.4445	0.4024	0.3934	11.3
3	0.1746	0.1616	0.1658	26.0
4	0.1094	0.1023	0.0988	33.1
5	0.0899	0.0759	0.0759	54.0

Because spatial information of feature map is consistent with the original image, CompCode is sensitive to variations within intra-palms such as translations and rotations. Thus, the translation operation, which allows brute force matching within a local range, can mitigate the misalignment to some extent. This capacity is demonstrated by the performance gap between results with and without template translation procedure for matching.

Moreover, the experiment, which uses three samples of each palm for training and the rest for testing, produces about 0.34 billion sample pairs during the matching stage. With the translation shift steps t, it can generate $(2t+1)^2 - 1$ times more matching per sample pair, strongly affecting the time consumption of palmprint recognition. The time consumption of the matching stage under different translation shift steps is listed in the final column of Table 8. As can be seen, the time consumption increased considerably as the increasing of translation shift steps. Actually, compared to the performance obtained with translation shift steps of 5, the performance of translation steps 6 increased slightly while the running

time increases sharply. Thus, Table 8 does not present the results of steps 6. With a comprehensive consideration of both the recognition performance and time consumption, the Gabor filter bank with 6 orientations, translation steps 5, and matching without rotations, are the optimal hyper-parameters of the CompCode for palmprint recognition on the CUHKSZ database.

Comparison and Analysis of Different Methods

In this experiment, a comparison of recognition methods is conducted between CompCode and some widely used palmprint methods including CR_CompCode (Zhang et al., 2017), RLOC (Jia et al., 2008), OLOF (Sun et al., 2005), LLDP with Gabor filters (LLDP-G) (Luo et al., 2016), and LLDP with MFRAT (LLDP-M) (Luo et al., 2016). Codes of these methods are provided by their authors. Considering the experimental time consumption on large-scale datasets, this chapter modifies the original code in a multithreading manner to reduce the running time in an acceptable scope. For a fair comparison, the parameters of these methods are in the default settings as their original paper. Different from the pixel-to-pixel strategy used in other methods, the palmprint matching strategy in RLOC is based on the pixel-to-area comparison. Specifically, in this experiment, RLOC uses the matching strategy of pixel-to-cross-shaped area comparison which is proven better than the pixel-to-small-square area comparison (Jia et al., 2008). Note that all the methods are conducted on the CUHKSZ palmprint dataset (only the palmprint modal is used), the results are shown in Table 9.

Table 9. Comparison of different methods on the CUHKSZ palmprint dataset

Recognition Methods	EER (%)
CompCode	**0.0759**
CR_CompCode	0.8062
LLDP-G	0.2875
LLDP-M	0.7642
OLOF	2.9361
RLOC	3.7150

Multi-Biometric Performance Comparison

To date, face and fingerprint biometrics recognition are the most widely used biometric techniques. To demonstrate the advantages of palmprint recognition, the CUHKSZ face dataset and the CUHKSZ fingerprint dataset are used to perform verification experiments.

Considering the over-fitting issues existing in deep learning methods, this experiment only chooses the conventional methods to test the recognition capability of different biometrics. Further, the parameters of each algorithm have been optimized to avoid the performance bias caused by improper algorithm parameters. The EERs are shown in Table 10. As can be seen, palmprint recognition achieved the lowest EER. Particularly, EER of 0.076% for palmprint recognition, while EER of 0.037% for bimodal (palmprint and palm vein) recognition. Note that for palmprint verification, the following parameters (k=6, t=5, r=0) were used with acceptable time consumption.

Table 10. Performance comparison of palmprint, face, and fingerprint recognition

CUHKSZ Dataset	Modal Type	No. of Classes	No. of Images	Methods	EER (%)
Palmprint (touchless)	Palmprint	20,000	120,000	CompCode	0.076
	Palm vein	20,000	120,000	CompCode	0.279
	Palmprint + Palm vein	20,000	120,000	Score Fusion	0.037
Face	Regular Face	4,000	8,000	HOG	2.075
	Large Deflection Angle	6,000	12,000	LBPH	4.026
Fingerprint	Thumb	20,000	100,000	Cappeli	1.718

FUTURE RESEARCH DIRECTIONS

Nowadays, issues and challenges raised in palmprint image sensing and recognition have become hot topics in TLPR. The large-scale palmprint dataset acquired in unconstrained environments intrinsically contain these factors and will offer unparalleled opportunities to researchers in the biometrics community. Accordingly, the future research directions of palmprint recognition are as follows:

- Unsupervised model: At present, the CNN-based palmprint feature extraction networks will be affected by the number of categories in the classification layer. Therefore, the generalization ability is limited. How to avoid interference from the classification loss to the feature encoding network module during training and how to design an unsupervised palmprint texture representation model are the focuses of future research;
- Palmprint IQA: Touchless palmprint IQA is the foundation of palmprint recognition in real-world applications. During the palmprint collection process, problems such as defocus blur, motion blur, and abnormal brightness may occur due to the change in the users' palm postures and positions. Palmprint quality indicators, such as brightness, sharpness, and illumination uniformity, can be used to further improve the accuracy and robustness of the palmprint recognition system;
- End-to-end model: How to integrate the current ROI keypoint detection, feature extraction, and recognition methods to achieve end-to-end palmprint recognition neural networks is one of the promising research directions.

CONCLUSION

During the last two decades, great progress has been made in touchless palmprint recognition. This chapter first elaborates on the basic definitions and challenges of touchless palmprint recognition. Then, this chapter introduces a subject-aligned large-scale multi-biometric dataset (CUHKSZ), which contains a considerable large-scale touchless palmprint subset, to thoroughly test the generalization ability of the touchless palmprint recognition technique. The experimental results on CUHKSZ show that parameter optimization brings enhanced performance and is considerably important to the final EER. To our best knowledge, no works on parameter optimization of CompCode on large-scale databases has been reported. The performance-changing trends can provide references for optimizations of other methods on large-scale datasets. Finally, to avoid the bias caused by a single algorithm, the performances of various palmprint recognition methods are compared. In addition, the multi-biometric experiment performed on

CUHKSZ palmprint, face, and fingerprint datasets demonstrates the advantage of touchless palmprint recognition in accuracy and provides useful guidance for civil applications.

REFERENCES

Afifi, M. (2019). 11K Hands: Gender recognition and biometric identification using a large dataset of hand images. *Multimedia Tools and Applications*, *78*(15), 20835–20854. doi:10.100711042-019-7424-8

Charfi, N., Trichili, H., Solaiman, B., & Alimi, A. M. (2021). *REST database* [Data set]. doi:10.21227/7gf6-v687

Chinese Academy of Sciences. (2005). *CASIA Palmprint Image Database* [Data set]. http://biometrics.idealtest.org/dbdetailforuser.do?id=5

Chinese Academy of Sciences. (2007). *CASIA Multi-Spectral Palmprint Database* [Data set]. http://biometrics.idealtest.org/dbdetailforuser.do?id=5#/datasetdetail/6

COEP Technological University. (2010). *COEP Palm Print Database* [Data set]. https://www.coep.org.in/resources/coeppalmprintdatabase

Delhi, I. I. T. (2008). *IIT Delhi Touchless Palmprint Database (Version 1.0)* [Data set]. https://www4.comp.polyu.edu.hk/~csajaykr/IITD/Database_Palm.htm

Fei, L., Lu, G., Jia, W., Teng, S., & Zhang, D. (2018). Feature extraction methods for palmprint recognition: A survey and evaluation. *IEEE Transactions on Systems, Man, and Cybernetics. Systems*, *49*(2), 346–363. doi:10.1109/TSMC.2018.2795609

Genovese, A., Piuri, V., Plataniotis, K. N., & Scotti, F. (2019). PalmNet: Gabor-PCA convolutional networks for touchless palmprint recognition. *IEEE Transactions on Information Forensics and Security*, *14*(12), 3160–3174. doi:10.1109/TIFS.2019.2911165

Genovese, A., Piuri, V., & Scotti, F. (2014). *Touchless palmprint recognition systems*. Springer Cham. doi:10.1007/978-3-319-10365-5

Jain, A. K., & Feng, J. (2008). Latent palmprint matching. *IEEE Transactions on Pattern Analysis and Machine Intelligence*, *31*(6), 1032–1047. doi:10.1109/TPAMI.2008.242 PMID:19372608

Jia, W., Hu, R.-X., Gui, J., Zhao, Y., & Ren, X.-M. (2012). Palmprint recognition across different devices. *Sensors (Basel)*, *12*(6), 7938–7964. doi:10.3390120607938 PMID:22969380

Jia, W., Huang, D.-S., & Zhang, D. (2008). Palmprint verification based on robust line orientation code. *Pattern Recognition*, *41*(5), 1504–1513. doi:10.1016/j.patcog.2007.10.011

Jia, W., Zhang, B., Lu, J., Zhu, Y., Zhao, Y., Zuo, W., & Ling, H. (2017). Palmprint recognition based on complete direction representation. *IEEE Transactions on Image Processing*, *26*(9), 4483–4498. doi:10.1109/TIP.2017.2705424 PMID:28541201

Kong, A., Zhang, D., & Kamel, M. (2009). A survey of palmprint recognition. *Pattern Recognition*, *42*(7), 1408–1418. doi:10.1016/j.patcog.2009.01.018

Kong, A.-K., & Zhang, D. (2004). Competitive coding scheme for palmprint verification. In *Proceedings of the 17th International Conference on Pattern Recognition (ICPR'04)*. IEEE. 10.1109/ICPR.2004.1334184

Kong, W. K., & Zhang, D. (2002). Palmprint texture analysis based on low-resolution images for personal authentication. *International Conference on Pattern Recognition*, *3*, 807-810. 10.1109/ICPR.2002.1048142

KTU CVPR Lab. (2015). *KTU Contactless Palmprint Database* [Data set]. https://ceng2.ktu.edu.tr/cvpr/contactlessPalmDB.htm

Liang, X., Fan, D., Yang, J., Jia, W., Lu, G., & Zhang, D. (2023). PKLNet: Keypoint localization neural network for touchless palmprint recognition based on edge-aware regression. *IEEE Journal of Selected Topics in Signal Processing*, 1–15. Advance online publication. doi:10.1109/JSTSP.2023.3241540

Liang, X., Li, Z., Fan, D., Li, J., Jia, W., & Zhang, D. (2022). Touchless palmprint recognition based on 3D Gabor template and block feature refinement. *Knowledge-Based Systems*, *249*, 108855. doi:10.1016/j.knosys.2022.108855

Liang, X., Li, Z., Fan, D., Zhang, B., Lu, G., & Zhang, D. (2022). Innovative contactless palmprint recognition system based on dual-camera alignment. *IEEE Transactions on Systems, Man, and Cybernetics. Systems*, *52*(10), 6464–6476. doi:10.1109/TSMC.2022.3146777

Liang, X., Yang, J., Lu, G., & Zhang, D. (2021). CompNet: Competitive neural network for palmprint recognition using learnable Gabor kernels. *IEEE Signal Processing Letters*, *28*, 1739–1743. doi:10.1109/LSP.2021.3103475

Liang, X., Zhang, D., Lu, G., Guo, Z., & Luo, N. (2021). A novel multicamera system for high-speed touchless palm recognition. *IEEE Transactions on Systems, Man, and Cybernetics. Systems*, *51*(3), 1534–1548. doi:10.1109/TSMC.2019.2898684

Luo, Y.-T., Zhao, L.-Y., Zhang, B., Jia, W., Xue, F., Lu, J.-T., Zhu, Y.-H., & Xu, B.-Q. (2016). Local line directional pattern for palmprint recognition. *Pattern Recognition*, *50*, 26–44. doi:10.1016/j.patcog.2015.08.025

Matkowski, W. M., Chai, T., & Kong, A. W. K. (2019). Palmprint recognition in uncontrolled and uncooperative environment. *IEEE Transactions on Information Forensics and Security*, *15*, 1601–1615. doi:10.1109/TIFS.2019.2945183

Sun, Z., Tan, T., Wang, Y., & Li, S. Z. (2005). Ordinal palmprint represention for personal identification [represention read representation]. In *Proceedings of the IEEE Computer Society Conference on Computer Vision and Pattern Recognition (CVPR'05)*. IEEE.

The Hong Kong Polytechnic University. (2003). *PolyU Palmprint Database* [Data set]. https://www4.comp.polyu.edu.hk/~biometrics

The Hong Kong Polytechnic University. (2009). *PolyU Multispectral Palmprint Database* [Data set]. https://www4.comp.polyu.edu.hk/~biometrics/MultispectralPalmprint/MSP.htm

University of Las Palmas de Gran Canaria. (2011). *GPDS100Contactlesshands2Band Database* [Data set]. https://gpds.ulpgc.es/

Zhang, D., Kong, W.-K., You, J., & Wong, M. (2003). Online palmprint identification. *IEEE Transactions on Pattern Analysis and Machine Intelligence*, *25*(9), 1041–1050. doi:10.1109/TPAMI.2003.1227981

Zhang, D., & Shu, W. (1999). Two novel characteristics in palmprint verification: Datum point invariance and line feature matching. *Pattern Recognition*, *32*(4), 691–702. doi:10.1016/S0031-3203(98)00117-4

Zhang, L., Cheng, Z., Shen, Y., & Wang, D. (2018). Palmprint and palmvein recognition based on DCNN and a new large-scale contactless palmvein dataset. *Symmetry*, *10*(4), 78. doi:10.3390ym10040078

Zhang, L., Li, L., Yang, A., Shen, Y., & Yang, M. (2017). Towards contactless palmprint recognition: A novel device, a new benchmark, and a collaborative representation based identification approach. *Pattern Recognition*, *69*, 199–212. doi:10.1016/j.patcog.2017.04.016

Zhong, D., Du, X., & Zhong, K. (2019). Decade progress of palmprint recognition: A brief survey. *Neurocomputing*, *328*, 16–28. doi:10.1016/j.neucom.2018.03.081

ADDITIONAL READING

Zhang, D., Guo, Z., & Gong, Y. (Eds.). (2015). *Multispectral biometrics: Systems and applications*. Springer Cham.

Zhang, D., Jing, X., & Yang, J. (Eds.). (2006). *Biometric image discrimination technologies*. IGI Global. doi:10.4018/978-1-59140-830-7

Zhang, D., & Lu, G. (Eds.). (2013). *3D Biometrics: Systems and Applications*. Springer Cham. doi:10.1007/978-1-4614-7400-5

Zhang, D., Lu, G., & Zhang, L. (Eds.). (2018). *Advanced biometrics*. Springer Cham. doi:10.1007/978-3-319-61545-5

Zhang, D., Song, F., Xu, Y., & Liang, Z. (Eds.). (2009). *Advanced pattern recognition technologies with applications to biometrics*. IGI Global. doi:10.4018/978-1-60566-200-8

Zhang, D., Xu, Y., & Zuo, W. (Eds.). (2016). *Discriminative learning in biometrics*. Springer Singapore. doi:10.1007/978-981-10-2056-8

Zhang, D. D. (Ed.). (2000). *Automated biometrics: Technologies and systems*. Springer New Yrok. doi:10.1007/978-1-4615-4519-4

Zhang, D. D. (Ed.). (2004). *Palmprint authentication*. Springer New Yrok.

KEY TERMS AND DEFINITIONS

Bimodal Palmprint Recognition: The recognition is based on images captured under two different ranges of light spectrum such as the visible and infrared light spectrum.

Multispectral Palmprint Recognition: The recognition is based on multispectral palmprint images which are captured by illuminating the palm with light sources of different spectral ranges.

Palm Vein Recognition: The process to identify a person using the palm vein textures which are formed by the subcutaneous veins of the palm.

Palmprint Image Alignment: For two palmprint images captured from the same palm, the process of mapping the probe image to the view plane of the reference image according to the projection mapping relationship established through the set of corresponding points detected from the two palmprint images. Generally, palmprint alignment is used to further reduce variations within intra-class samples.

Palmprint Image Preprocessing: A series of processing performed on a palmprint image to obtain an image suitable for feature extraction. Generally, it includes palm region segmentation, palm keypoint localization, ROI localization, normalization, palmprint image quality assessment, and enhancement.

Palmprint Keypoint Localization: The process of determining the locations of the keypoints of a palm in an image, in which the keypoints are a sequence of points in a palmprint image that is physically and geometrically distinctive for palmprint ROI localization.

Palmprint Principal Lines: The deepest and thickest lines on the palm, also known as the distal, radial, and proximal creases or the heart, head, and life lines of the palm.

Palmprint Region of Interest (ROI): The palm area, mostly the center area of the palm side, is used to extract palmprint features and perform identity recognition.

Palmprint Template: A structural data unit recording the extracted palmprint features and related auxiliary information, such as the algorithm used for feature extraction and the quality indicator of the input palmprint image.

ROI Localization: The process of determining the location of the palmprint ROI. Palmprint ROI localization, as a geometric normalization operation, is performed to reduce translation, rotation, and scale variations between different palmprint images.